Inorganic Chemistry

Article

Cite This: *Inorg. Chem.* 2019, 58, 13440−13445

pubs.acs.org/IC

Two Kinds of Metastable Structures in an Epitaxial Lanthanum Cobalt Oxide Thin Film

Xiangxiang Guan,[†,‡] Xi Shen,[†] Weipeng Wang,[†] Wei Wang,[†,‡] Qianqian Lan,[†] Jing Zhang,[†,‡] Jine Zhang,[†,‡] Huaiwen Yang,[†,‡] Yuan Yao,[†] Junjie Li,[†] Changzhi Gu,[†,‡] Jirong Sun,[†,‡] and Richeng Yu*[,†,‡]

[†]Beijing National Laboratory of Condensed Matter Physics, Institute of Physics, Chinese Academy of Sciences, Beijing 100190, P. R. China

[‡]School of Physical Sciences, University of Chinese Academy of Sciences, Beijing 100049, P. R. China

Supporting Information

ABSTRACT: Thin films have attracted much interest because they often have novel properties different from those of their bulk counterparts. In this work, we tune two metastable states in three kinds of lanthanum cobalt oxide thin films by electron beam irradiation and record their dynamic transition process in situ in a transmission electron microscope. The lanthanum cobalt oxide thin films exhibit a homogeneous microstructure in the initial state and then transfer to a stripelike superstructure with $3a_0$ periodicity (a_0 is the perovskite lattice parameter), further developing into a superstructure with $2a_0$ periodicity in dark stripes (brownmillerite structure). To explore the inherent energy discrepancy within the two metastable states, we perform first-principles calculations on a $LaCoO_{3-\delta}$ ($0 \leq \delta \leq 0.5$) thin film system by geometry optimization. The calculation results suggest that the forming energy of the $3a_0$ periodicity stripelike structure is a little lower than that of the $2a_0$ periodicity in the $LaCoO_{3-\delta}$ thin film. Our work explains why the two stripelike structures coexist in lanthanum cobalt oxide thin films and extends prospective applications related to oxygen vacancies in thin films.

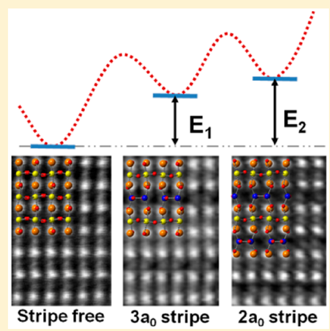

INTRODUCTION

Any substance in nature is in its minimum energy state. All of the systems we observed are the equilibrium results of two or more energy competitions. For instance, the battle of long-range order and disorder (short-range order) at lattice dimension forms an amorphous structure.[1−3] Superconductivity is the form of the competition between thermoenergy and electron migration.[4,5] In particular, in strongly electron-correlated systems, all of the observed intriguing functionalities and phases are in the stable or metastable states stemming from the competitions among electron, lattice, orbital, and spin under external disturbances such as temperature and pressure.[6−8]

An epitaxial transition-metal oxide thin film is a remarkably metastable existence influenced by several competing factors. The mismatch between the lattices of the substrate and epitaxial film induces a strain energy that reaches a maximum residing at the interface and expands to the whole film.[9−11] The strain energy competes with the crystal field energy of the film, which gives rise to the change in the spin states of the transition-metal ions. When a transition-metal oxide film is observed in a transmission electron microscope (TEM), electron beam irradiation (EBI) as an external tool can intentionally tailor the oxygen concentrations through the knock-on effect.[12−14] Moreover, the heterostructure grouping of at least two kinds of materials in a thin film would produce novel physical properties. For instance, electron reconstruction occurring at the interface of $LaMnO_3/SrTiO_3$ heterostructure provokes the emergency of magnetism.[15] By coupling a fixed thick $La_{0.7}Sr_{0.3}MnO_3$ layer with a varying-thickness $LaCoO_3$ layer, Thota et al. demonstrated that interfacial ferromagnetic coupling is enhanced upon decreasing the thickness of $LaCoO_3$.[16]

Recently, lanthanum cobalt oxide thin films have attracted considerable attention because of their fantastic physical properties related to their prolific stripelike structures.[16−20] The epitaxial $La_{1-x}A_xCoO_{3-\delta}$ (A is a rare earth element, $0 \leq x \leq 1$, $0 \leq \delta \leq 0.5$) thin film exhibits numerous complicated oxygen vacancy orderings.[21−26] Taking the $LaCoO_{3-\delta}$ thin film grown on $SrTiO_3$ (STO) as an example, Zhang et al. observed the superstructure with $3a_0$ periodicity in dark stripes,[26] whereas Jang et al. reported the superstructures with $2a_0$ and $3a_0$ periodicities in dark stripes.[27] (Here, $2a_0$ is the periodicity of the occurrence of a dark stripe though the neighbor dark stripes are not equivalent, whose crystal structure possesses a brownmillerite phase with a periodicity of $4a_0$ perpendicular to the dark stripes. $3a_0$ is the periodicity of the occurrence of a dark stripe, whose crystal structure adopts an intermediate phase between the perovskite phase and the brownmillerite phase, with a periodicity of $3a_0$ perpendicular to the dark stripes. Hereafter, we call them $2a_0$ and $3a_0$, respectively.)

Received: August 1, 2019
Published: September 26, 2019

DOI: 10.1021/acs.inorgchem.9b02326
Inorg. Chem. 2019, 58, 13440−13445

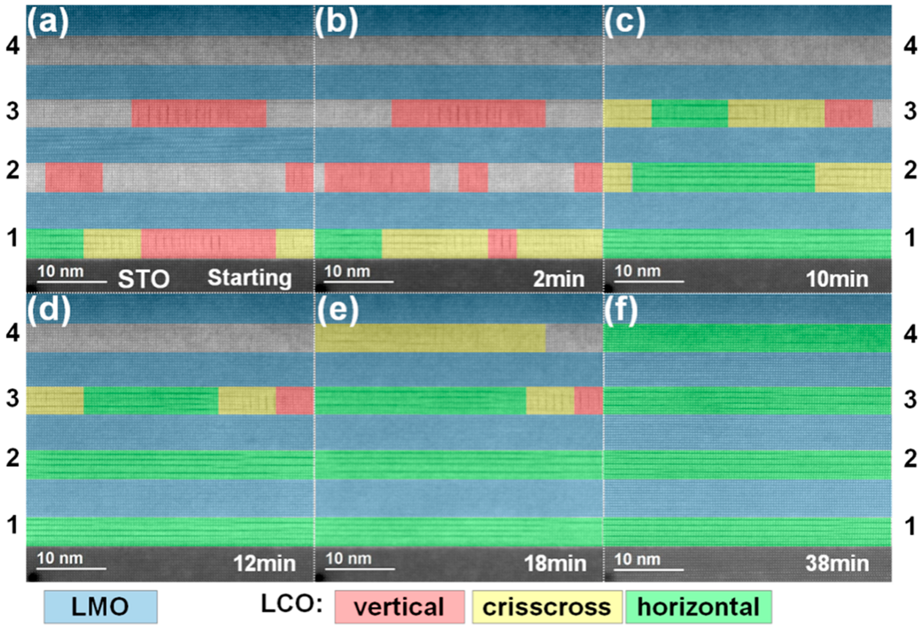

Figure 1. Sequence of the HAADF images of LCO/LMO SL along the [100] zone axis subjected to EBI. The images of LCO/LMO SL were recorded (a) at the beginning of the experiment and after being irradiated for (b) 2, (c) 10, (d) 12, (e) 18, and (f) 38 min, respectively. The LMO layers are colored blue. The LCO layers with vertical dark stripes, horizontal dark stripes, and crisscrossed dark stripes are colored green, yellow, and red, respectively. The LCO layers are numbered "1" to "4" on the side of the images.

Moreover, the dark stripes are either parallel or perpendicular to the interface between the film and the substrate.[23] Our previous studies also show that the dark stripes with periodicities of both $2a_0$ and $3a_0$ coexist in $La_{1-y}Sr_yCoO_3$ ($0 \leq y \leq 0.1$) and $La_{0.9}Ca_{0.1}CoO_{3-\delta}$ thin film systems.[19,28]

The morphology in lanthanum cobalt oxides is very changeable. However, the previous investigation of the structural evolution of lanthanum cobalt oxide merely focused on the $LaCoO_3/SrTiO_3$ superlattice.[27] Moreover, the origin of the coexistence of different morphologies in the same lanthanum cobalt oxide film system is still unclear. Furthermore, the forming energy of stripelike structure with the $2a_0$ or $3a_0$ periodicity in the lanthanum cobalt oxide thin film has not been reported.

In this work, to obtain a general rule for the structural evolution in lanthanum cobalt oxides, we investigate an electron-beam-irradiation-induced structural transition between $2a_0$ and $3a_0$ periodicity dark stripes in three lanthanum cobalt oxide thin film systems by using a JEOL ARM200 TEM with double Cs correctors. Electron energy loss spectroscopy (EELS) is employed to measure the oxygen concentration in the dark stripe. The calculations of the forming energies reveal the energy stabilities of $2a_0$ and $3a_0$ stripelike structures in a tensile/compressive strained thin film. Our work shows that altering the periodicity of the dark stripes and controlling their orientation can be realized by EBI and provides a clear energy scene of the $2a_0$ and $3a_0$ stripelike structures in $LaCoO_{3-\delta}$ thin films.

■ EXPERIMENTAL SECTION

Sample Fabrication. Three different thin film systems were fabricated by a pulsed-laser deposition method. They are a superlattice (SL) with alternately stacked $LaCoO_3$ (LCO) and $LaMnO_3$ (LMO) layers on a [100]-oriented STO substrate, a trilayer consisting of 5-nm-thick $La_{0.67}Sr_{0.33}MnO_3$ (LSMO) sandwiched by two layers of 7-nm-thick $La_{0.8}Sr_{0.2}CoO_3$ (LSCO) epitaxially grown on STO substrate, and a single layer with 35/70-nm-thick $La_{0.9}Ca_{0.1}CoO_3$ (LCCO) thin films on the STO substrate. The details of thin film fabrication can be found in our previous papers.[29−31]

TEM Characterization. All of the TEM lamellas were prepared with a focused ion beam Helios 600i. A TEM study was performed at 200 keV on a JEM-ARM200F with double aberration correctors. The STEM mode conditions for irradiating the samples are listed in Supporting Information Table S1. All of the original high-angle annular dark-field (HAADF) images are 1024 × 1024 pixels in size. EELS line scans were acquired in steps of 2 Å. The spot size was set to be 6C, and each point had a duration time of 0.1 s to gain enough counts and good stability simultaneously. Dual EELS mode was employed to obtain a real-time zero loss peak for the correction of the zero/core loss peak drift and also to remove the plural scattering effect.

First-Principles Calculation. The CASTEP modus was exploited to execute the geometry optimization with restrictions in $LaCoO_{3-\delta}$ thin films and to calculate the final energy. A gradient-corrected form of the exchange-correlation function (generalized gradient approximation (GGA-PBE)) was used.[32] The details of the restrictions for the thin films are presented in the main text. The crystal symmetry was set to P1 for geometry optimization. The oxygen molecule model was made by setting two oxygen atoms with a bond length of 1.209 Å into a 10 × 10 × 10 $Å^3$ crystal frame.

■ RESULTS AND DISCUSSION

EBI-Induced Structural Evolution. Figure 1 shows the structural evolution of LCO/LMO SL under EBI over the whole image area. In the initial state (Figure 1a), the vertical (perpendicular to the plane of substrate) and horizontal (parallel to the plane of substrate) dark stripes or crisscrosses existed in the inner LCO layers (labeled as "1", "2", "3" in Figure 1). Meanwhile, the structure without stripes dominates the outermost LCO layer (labeled as "4" in Figure 1). When the SL was exposed to the focused electron beam with a spot size of 6C (as shown in Table S1), alterations of the nanostructures of LCO layers in SL take place. The effect of electron beam irradiation on an LCO thin film versus time has

DOI: 10.1021/acs.inorgchem.9b02326
Inorg. Chem. 2019, 58, 13440−13445

several stages as shown in Figure 1b−f: First, areas of vertical dark stripes become dense and expand laterally. Second, vertical dark stripes turn into crisscrossed dark stripes and finally develop into horizontal dark stripes. These evolutions indicate a nucleation process, and the extent of the nucleation is larger in the bottom LCO layer than in the outer LCO layers. In general, the areas of the dark stripes are enlarging with a gradually increasing dose of EBI.

To study the structural evolution in detail, the magnified HAADF images from LCO layer 1 are shown in Figure 2.

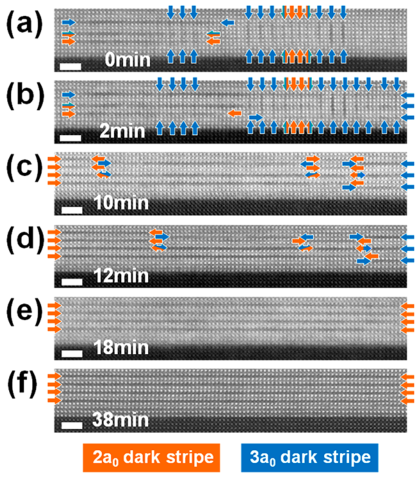

Figure 2. Magnified HAADF images cut from LCO layer 1. With increasing the dose of EBI, the periodicity of the dark stripes in the LCO layer changes from $3a_0$ to $2a_0$. Scale bar: 2 nm.

Initially, vertical dark stripes and horizontal dark stripes coexist in layer 1. The structure of the vertical dark stripes has a periodicity of $3a_0$, while on the left, the structure of horizontal dark stripes has mixed periodicities of $2a_0$ and $3a_0$ (Figure 2a). With gradually increasing the time of EBI, all of the $3a_0$ dark stripes structure become $2a_0$ stripes (Figure 2f). It should be noted that there is a competition between $2a_0$ and $3a_0$ periodicities of the stripelike structures, which can be seen in Figure 2c−e. As for the outer part of the thin film, in addition to being relatively slower, LCO in layer 3 has a similar tendency in the evolution of dark stripes shown in Supporting Information Figure S1.

To explore the general rule of the structural evolution in lanthanum cobalt oxides, we also investigate LSCO and LCCO in trilayer and single-layer thin films. The structural evolution of the LSMO/LSCO/LSMO trilayer thin film is shown in Supporting Information Figure S2. The EBI causes two kinds of changes in the lattice image of LSCO. The first one is that the original structure without a stripe is transformed into a structure of interlacing dark stripes with $2a_0$ and $3a_0$ periodicities (red areas in Supporting Information Figure S2a−c), and the second one is the formation of completely horizontal dark stripes with a $3a_0$ periodicity from the initial horizontal and vertical staggered dark stripes with a $3a_0$ periodicity (as shown in yellow areas in Supporting Information Figure S2d−f).

In the case of the lightly doped lanthanum cobalt oxide $La_{0.9}Ca_{0.1}CoO_3$ (LCCO) thin films in Supporting Information Figure S3, as the duration of EBI increases, the $3a_0$ periodicity of vertical dark stripes gradually forms and then subsequently transform into either $2a_0$ periodicity vertical dark stripes interspersed with a few horizontal dark stripes in a 35-nm-thick LCCO thin film or into mixed vertical dark stripes with $2a_0$ and $3a_0$ periodicities in a LCCO thin film with a thickness of 70 nm. The final features stay unchanged under EBI at long-enough time.[28]

To summarize the behavior of the above three lanthanum cobalt oxide thin film systems, we can conclude that all of the thin films can change from a stripe-free structure to a $3a_0$ horizontal and/or vertical dark stripe structure and subsequently transform into a $2a_0$ horizontal and/or vertical dark stripe structure under EBI. It demonstrates that the dark stripe structure with $2a_0$ periodicity is more difficult to form than that with $3a_0$ periodicity.

Oxygen Vacancies in $2a_0$ and $3a_0$ Stripelike Structures by EELS. It is well known that EBI can introduce oxygen vacancies into metal oxides through knock-on effects.[33,34] To explore the oxygen-deficient states in lanthanum cobalt oxide thin films, we carried out EELS studies and present the EELS O−K edges at dark stripes and bright stripes (next to dark stripes) of LCO in an LCO/LMO SL thin film in Figure 3. The O−K edge structure in the EELS

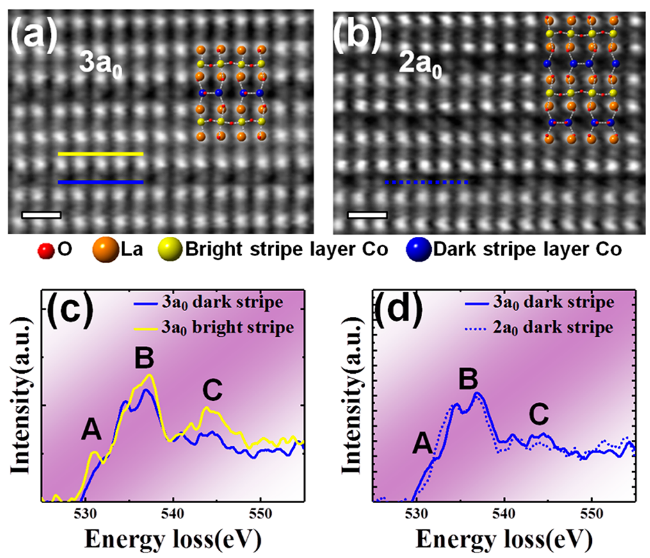

Figure 3. EELS O−K edges of $3a_0$ and $2a_0$ periodicities dark stripe structures. [110] zone-axis-view HAADF images of dark stripe structures with (a) $3a_0$ periodicity and (b) $2a_0$ periodicity overlapped with the projection models of $LaCoO_{2.67}$ and $LaCoO_{2.5}$, respectively. (c) EELS line-scan O−K edges of a dark stripe and bright stripe in (a) at LCO layers in an LCO/LMO SL thin film. Blue and yellow lines in (a) indicate the specific locations of dark and bright stripes for the EELS line scan, respectively. (d) EELS line-scan O−K edges of dark stripes in a stripelike structure with $3a_0$ periodicity (a) as shown by the solid blue line and that with $2a_0$ periodicity (b) as shown by the dotted blue line.

spectrum offers information on the electron excitations from the O 1s orbital to the 2p orbitals. Three basic features labeled A−C can be found in Figure 3c,d, corresponding to the hybridization of O 2p with Co 3d, La 5d, and Co 4sp, respectively. As one can see from Figure 3c, the intensities of all three peaks in dark stripes are lower than those in bright stripes, especially prepeak A, which is a characteristic feature for positive correlation with the valence of Co.[35,36] By analyzing the oxygen prepeaks in $3a_0$ stripelike structure, we found that the dark stripes have a significant oxygen vacancy

DOI: 10.1021/acs.inorgchem.9b02326
Inorg. Chem. 2019, 58, 13440−13445

comparing to bright stripes. As for the stripelike structure with $2a_0$ periodicity, the dark stripe has an oxygen deficiency similar to that in the $3a_0$ periodicity structure (Figure 3d), indicating that the stripelike structure with $2a_0$ periodicity has more oxygen deficiency than that with $3a_0$ periodicity for the same large area. In addition, LCCO and LSCO systems show similar results. Moreover, the Co ions in the dark stripes with both $3a_0$ periodicity and $2a_0$ periodicity along the [110] direction have a breathing mode which agrees with the projection views of $LaCoO_{2.67}$ and $LaCoO_{2.5}$ (Figure 3a,b). According to the above analyses, we take the crystal structures of $LaCoO_{2.5}$ and $LaCoO_{2.67}$ as the approximate prototypes for the $2a_0$ and $3a_0$ stripelike structures, respectively.

Forming Energy of $LaCoO_{3-\delta}$ in a Thin Film. To determine the nature of the energy of these metastable structures in thin film systems, we carried out first-principles calculations by using previously mentioned bulk crystal structures of $LaCoO_3$, $LaCoO_{2.5}$, and $LaCoO_{2.67}$ as starting structures for the stripe-free structure and $2a_0$ and $3a_0$ stripelike structures, respectively.[37−39] In this study, we apply the lattice parameter of the STO substrate (as shown in Figure 4a−e) to that of $LaCoO_{3-\delta}$ thin films along the two in-plane directions, release the out-of-plane lattice, and set all of the axial angles equal to 90° simultaneously. To clearly present the settings, we exhibit the related models of the atomic arrangement along the out-of-plane direction in Figure 4f−j.

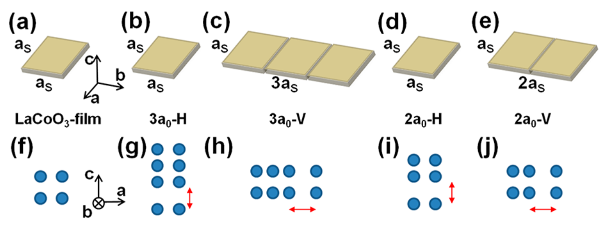

Figure 4. In-plane and out-of-plane views of (a, f) the $LaCoO_3$ film; (b, g; in short "$3a_0$-H") the $3a_0$ horizontal stripelike structure; (c, h; in short "$3a_0$-V") the $3a_0$ vertical stripelike structure; (d, i; in short "$2a_0$-H") the $2a_0$ horizontal stripelike structure; and (e, j; in short "$2a_0$-V") the $2a_0$ vertical stripelike structure thin films. Light-brown squares represent the lattice grids in a−e. Blue circles refer to the La atoms in f−j.

The previous investigations on bulk $LaCoO_{2.5}$ and $LaCoO_{2.67}$ were limited to equilibrium lattice constants and volumes without optimizing the internal parameters.[38,39] In this work, through the geometry optimizations by the CASTEP modus, we obtain the final energies of $LaCoO_3$, $LaCoO_{2.5}$, and $LaCoO_{2.67}$ thin films by performing a full optimization of the lattice parameters and the atomic coordinates in the unit cell. The final energies of $LaCoO_3$-f, $3a_0$-H, $2a_0$-H, $3a_0$-V, and $2a_0$-V are presented in Table 1. In addition, to ascertain the energy stabilities between the $2a_0$ and $3a_0$ stripe-like structure in thin films, we calculate the forming energies (E_1 for $LaCoO_{2.67}$, E_2 for $LaCoO_{2.5}$), which are also shown in Table 1, in conformity with eqs 1 and 2. The results lead to the following two conclusions: (1) No matter the direction of the dark stripe (i.e., horizontal or vertical), the dark stripe crystal structures with a same periodicity have very similar forming energy values. (2) The forming energy values for the dark stripe structures with $3a_0$ periodicity are slightly lower than that with $2a_0$ periodicity. The first result explains why the horizontal and vertical dark stripes are widely staggered in our $LaCoO_{3-\delta}$ thin films and why some places are horizontal whereas some other places are vertical in the previously reported $LaCoO_{3-\delta}$ thin films.[23,40] The second result confirms the order of appearance of dark stripes under EBI, namely, the $3a_0$ periodicity dark stripe appears at first and then transforms into the dark stripes with $2a_0$ periodicity. The result also depicts the rationality of the coexistence of the $2a_0$ and $3a_0$ periodicity dark stripes. We performed the calculations for the $LaCoO_{3-\delta}$ thin film not only on the tensile STO substrate but also on the compressive $LaAlO_3$ substrate. The result of $LaCoO_{3-\delta}$ on the $LaAlO_3$ substrate shows the same tendency as that on the STO substrate, as shown in Supporting Information Table S2. Nevertheless, our calculations merely concern the fixed strain from substrates. It is worth noticing that the coexistence of $2a_0$ and $3a_0$ periodicity horizontal/vertical stripelike structures may be attributed to the local stress induced by the epitaxial growth. When EBI is introduced, a competition between electron-beam-induced energy and local strain energy occurs. If the EBI effect is high enough, then the final state in $LaCoO_{3-\delta}$ will be shown as $2a_0$ periodicity dark stripes. Once the effects from EBI and local stress are comparable, the coexistence of $2a_0$ and $3a_0$ periodicity dark stripes easily emerges as observed in Figure 2. In other words, one metastable state can transform to another metastable state when it gets high enough energy from EBI to overcome the energy barrier between the two states. Besides, in our EBI experiment on LCO/LMO SL, the final state of the LCO shows horizontal dark stripes with $2a_0$ periodicity. It might be caused by the interfacial magnetic coupling as previously reported.[29]

$$LaCoO_3 \xrightarrow{+E_1} LaCoO_{2.67} + \frac{1}{6}O_2 \quad (1)$$

$$LaCoO_3 \xrightarrow{+E_2} LaCoO_{2.5} + \frac{1}{4}O_2 \quad (2)$$

Bulk $LaCoO_{2.5}$ is a G-type antiferromagnetic material in which Co atoms have two kinds of magnetic moment values and bulk $LaCoO_{2.67}$ orders antiferromagnetically with three kinds of magnetic moments for cobalt atoms.[38,39] The thin film counterpart usually has different physical properties compared to those of the bulk. For instance, bulk $LaCoO_3$ is nonmagnetic at low temperatures, but the epitaxial $LaCoO_3$ thin film shows a ferromagnetic property below ∼75 K.[41] Therefore, the $LaCoO_{3-\delta}$ thin films in our study are predicted to possess different physical properties compared to those of

Table 1. Forming Energies of the Metastable States in the $LaCoO_{3-\delta}$ ($0 \le \delta \le 0.5$) Thin Film on a Tensile STO Substrate

(eV/unit cell)	$LaCoO_3$ film	O_2	$3a_0$-H	$3a_0$-V	$2a_0$-H	$2a_0$-V
final energy	−38.610	−8.348	−35.839	−35.890	−34.368	−34.382
forming energy			1.380 (E_1^H)[a]	1.329 (E_1^V)[b]	2.155(E_2^H)[c]	2.141 (E_2^V)[d]

[a] E_1^H denotes the forming energy of the structure of a horizontal dark stripe with $3a_0$ periodicity. [b] E_1^V denotes the forming energy of the structure of a vertical dark stripe with $3a_0$ periodicity. [c] E_2^H denotes the forming energy of the structure of a horizontal dark stripe with $2a_0$ periodicity. [d] E_2^V denotes the forming energy of the structure of a vertical dark stripe with $2a_0$ periodicity.

DOI: 10.1021/acs.inorgchem.9b02326
Inorg. Chem. 2019, 58, 13440−13445

their bulk counterparts. As mentioned in our previous studies,[19,28] the magnetization of lanthanum cobalt oxides has a positive correlation with the number of dark stripes, so the magnetization of the $La_{0.9}Ca_{0.1}CoO_{3-\delta}$ thin film can be tuned via structural transitions by EBI.

CONCLUSIONS

This work shows that the EBI induces a dynamic evolution of dark stripe structures with $3a_0$ and $2a_0$ periodicities in LCO/LMO SL, the LSCO/LSMO/LSCO multilayer, and LCCO single-layer thin film systems by in situ TEM. During the EBI process, the coexistence of $2a_0$ and $3a_0$ periodicity dark stripes as well as vertical and horizontal dark stripes is widely observed. By analyzing the EELS O−K edges, we discovered that the concentration of oxygen vacancy in the $2a_0$ periodicity stripelike structure is higher than that in the $3a_0$ periodicity stripelike structure. By geometry optimization for $LaCoO_{3-\delta}$ ($0 \leq \delta \leq 0.5$) thin films with restrictions, we ascertain that the horizontal or vertical dark stripe structure with $3a_0$ periodicity has a priority to emerge compared to that with $2a_0$ periodicity on the basis of the forming energy. Moreover, the stripelike structures with a same periodicity have similar forming energy which is in accordance with the experimental results. Such a tiny energy discrepancy in $LaCoO_{3-\delta}$ provides the opportunity to switch the orientations and the numbers of dark stripes, which could modify the magnetization through altering the valence and spin states of Co ions as shown in our previous studies.[28] Our work explains the existence of different morphologies in lanthanum cobalt oxide thin film systems and makes it possible to tune their physical properties.

ASSOCIATED CONTENT

Supporting Information

The Supporting Information is available free of charge on the ACS Publications website at DOI: 10.1021/acs.inorgchem.9b02326.

EBI conditions for three thin film systems; EBI-induced structural evolutions for LCO layer 3 in LCO/LMO SL, LSCO/LSMO/LSCO, and LCCO thin films; and forming energy of $LaCoO_{3-\delta}$ in a thin film on a compressive $LaAlO_3$ substrate (PDF)

AUTHOR INFORMATION

Corresponding Author

*E-mail: rcyu@iphy.ac.cn.

ORCID

Xiangxiang Guan: 0000-0003-1148-2669
Jine Zhang: 0000-0001-7949-3239
Junjie Li: 0000-0002-1508-9891
Changzhi Gu: 0000-0002-2689-2807
Jirong Sun: 0000-0003-1238-8770
Richeng Yu: 0000-0002-8086-0910

Notes

The authors declare no competing financial interest.

ACKNOWLEDGMENTS

This work was supported by the National Key Research Program of China (grant nos. 2017YFA0206200, 2016YFA0300701, and 2018YFA0208402) and the National Natural Science Foundation of China (grant nos. 11574376, 11874413, and 11934017). X.S. is grateful for the support from the Youth Innovation Promotion Association of CAS (2019009).

REFERENCES

(1) Sheng, H. W.; Luo, W. K.; Alamgir, F. M.; Bai, J. M.; Ma, E. Atomic packing and short-to-medium-range order in metallic glasses. *Nature* **2006**, *439* (7075), 419−25.

(2) Shi, S.; Qian, S.; Hou, X.; Mu, J.; He, J.; Chou, X. Structural and Optical Properties of Amorphous Al_2O_3 Thin Film Deposited by Atomic Layer Deposition. *Adv. Condens. Matter Phys.* **2018**, *2018*, 1−10.

(3) Liu, Y. H.; Wang, G.; Wang, R. J.; Zhao, D. Q.; Pan, M. X.; Wang, W. H. Super Plastic Bulk Metallic Glasses at Room Temperature. *Science* **2007**, *315*, 1385−1388.

(4) Ren, Z. A.; Lu, W.; Yang, J.; Yi, W.; Shen, X. L.; Li, Z. C.; Che, G. C.; Dong, X. L.; Sun, L. L.; Zhou, F.; Zhao, Z. X. Superconductivity at 55 K in Iron-Based F-Doped Layered Quaternary Compound Sm[O1-xFx] FeAs. *Chin. Phys. Lett.* **2008**, *25* (6), 2215−2216.

(5) Mourik, V.; Zuo, K.; Frolov, S. M.; Plissard, S. R.; Bakkers, E. P. A. M.; Kouwenhoven, L. P. Signatures of Majorana Fermions in Hybrid Superconductor-Semiconductor Nanowire Devices. *Science* **2012**, *336*, 1003−1007.

(6) Greenberg, E.; Leonov, I.; Layek, S.; Konopkova, Z.; Pasternak, M. P.; Dubrovinsky, L.; Jeanloz, R.; Abrikosov, I. A.; Rozenberg, G. K. Pressure-Induced Site-Selective Mott Insulator-Metal Transition in Fe_2O_3. *Phys. Rev. X* **2018**, *8*, 031059.

(7) Tokura, Y.; Nahaosa, N. Orbital Physics in Transition-Metal Oxides. *Science* **2000**, *288*, 462−468.

(8) Dagotto, E.; Hotta, T.; Moreo, A. Colossal Magnetoresistant Materials: The Key Role of Phase Seperation. *Phys. Rep.* **2001**, *344*, 1−153.

(9) Thompson, C. V.; Roland, C. Stress and Grain Growth in Thin Films. *J. Mech. Phys. Solids* **1996**, *44*, 657−673.

(10) LeGoues, F. K.; Copel, M.; Tromp, R. Novel strain-induced defect in thin molecular-beam epitaxy layers. *Phys. Rev. Lett.* **1989**, *63* (17), 1826−1829.

(11) Ye, T.; Suo, Z.; Evans, A. G. Thin film cracking and the roles of substrate and interface. *Int. J. Solids Struct.* **1992**, *29* (21), 2639−2648.

(12) Nord, M.; Vullum, P. E.; Hallsteinsen, I.; Tybell, T.; Holmestad, R. Assessing electron beam sensitivity for $SrTiO_3$ and $La_{0.7}Sr_{0.3}MnO_3$ using electron energy loss spectroscopy. *Ultramicroscopy* **2016**, *169*, 98−106.

(13) Yao, L.; Majumdar, S.; Akaslompolo, L.; Inkinen, S.; Qin, Q. H.; van Dijken, S. Electron-beam-induced Perovskite-Brownmillerite-Perovskite structural phase transitions in epitaxial $La_{2/3}Sr_{1/3}MnO_3$ films. *Adv. Mater.* **2014**, *26* (18), 2789−93.

(14) Houben, L.; Heidelmann, M.; Gunkel, F. Spatial resolution and radiation damage in quantitative high-resolution STEM-EEL spectroscopy in oxides. *Micron* **2012**, *43* (4), 532−537.

(15) Chen, Z.; Chen, Z.; Liu, Z. Q.; Holtz, M. E.; Li, C. J.; Wang, X. R.; Lu, W. M.; Motapothula, M.; Fan, L. S.; Turcaud, J. A.; Dedon, L. R.; Frederick, C.; Xu, R. J.; Gao, R.; N'Diaye, A. T.; Arenholz, E.; Mundy, J. A.; Venkatesan, T.; Muller, D. A.; Wang, L.-W.; Liu, J.; Martin, L. W. Electron Accumulation and Emergent Magnetism in $LaMnO_3/SrTiO_3$Heterostructures. *Phys. Rev. Lett.* **2017**, *119*, 156801.

(16) Thota, S.; Roychowdhury, K.; Thakare, V.; Ganguli, S. C.; Chen, Z. H.; Guo, E. J.; Das, S. Structural and magnetic properties of $La_{0.7}Sr_{0.3}MnO_3/LaCoO_3$ heterostructures. *Appl. Phys. Lett.* **2018**, *113* (12), 122405.

(17) Liu, B.; Wang, Y.; Liu, G.; Feng, H.; Yang, H.; Sun, J. Electrical transport properties of $La_{1-x}Sr_xCoO_3$ thin films. *J. Appl. Phys.* **2016**, *120* (15), 154103.

(18) Liu, H.; Sun, H.; Xie, R.; Zhang, X.; Zheng, K.; Peng, T.; Wu, X.; Zhang, Y. Substrate-dependent structural and CO sensing properties of $LaCoO_3$ epitaxial films. *Appl. Surf. Sci.* **2018**, *442*, 742−749.

(19) Lan, Q. Q.; Shen, X.; Yang, H. W.; Zhang, H. R.; Zhang, J.; Guan, X. X.; Yao, Y.; Wang, Y. G.; Yu, R. C.; Peng, Y.; Sun, J. R.

Correlation between magnetism and "dark stripes" in strained $La_{1-x}Sr_xCoO_3$ epitaxial films ($0 \leq x \leq 0.1$). *Appl. Phys. Lett.* **2015**, *107* (24), 242404.
(20) Mefford, J. T.; Rong, X.; Abakumov, A. M.; Hardin, W. G.; Dai, S.; Kolpak, A. M.; Johnston, K. P.; Stevenson, K. J. Water electrolysis on $La_{1-x}Sr_xCoO_{3-\delta}$ perovskite electrocatalysts. *Nat. Commun.* **2016**, *7*, 11053.
(21) Biškup, N.; Salafranca, J.; Mehta, V.; Oxley, M. P.; Suzuki, Y.; Pennycook, S. J.; Pantelides, S. T.; Varela, M. Insulating FerromagneticLaCo$O_{3-\delta}$Films: A Phase Induced by Ordering of Oxygen Vacancies. *Phys. Rev. Lett.* **2014**, *112*, 087202.
(22) Gazquez, J.; Luo, W.; Oxley, M. P.; Prange, M.; Torija, M. A.; Sharma, M.; Leighton, C.; Pantelides, S. T.; Pennycook, S. J.; Varela, M. Atomic-resolution imaging of spin-state superlattices in nanopockets within cobaltite thin films. *Nano Lett.* **2011**, *11* (3), 973−6.
(23) Liu, G.; Li, X.; Wang, Y.; Liang, W.; Liu, B.; Feng, H.; Yang, H.; Zhang, J.; Sun, J. Nanoscale domains of ordered oxygen-vacancies in $LaCoO_3$ films. *Appl. Surf. Sci.* **2017**, *425*, 121−129.
(24) Mehta, V. V.; Biskup, N.; Jenkins, C.; Arenholz, E.; Varela, M.; Suzuki, Y. Long-range ferromagnetic order inLa$CoO_{3-\delta}$ epitaxial films due to the interplay of epitaxial strain and oxygen vacancy ordering. *Phys. Rev. B: Condens. Matter Mater. Phys.* **2015**, *91*, 144418.
(25) Van Overmeere, Q.; Baniecki, J. D.; Yamazaki, T.; Ricinschi, D.; Aso, H.; Miyata, Y.; Yamada, H.; Fujimura, N.; Kataoka, Y.; Imanaka, Y. Interface energetics and atomic structure of epitaxial $La_{1-x}Sr_xCoO_3$ on Nb:$SrTiO_3$. *Appl. Phys. Lett.* **2015**, *106* (24), 241602.
(26) Zhang, N.; Zhu, Y.; Li, D.; Pan, D.; Tang, Y.; Han, M.; Ma, J.; Wu, B.; Zhang, Z.; Ma, X. Oxygen Vacancy Ordering Modulation of Magnetic Anisotropy in Strained $LaCoO_{3-x}$ Thin Films. *ACS Appl. Mater. Interfaces* **2018**, *10*, 38230−38238.
(27) Jang, J. H.; Kim, Y. M.; He, Q.; Mishra, R.; Qiao, L.; Biegalski, M. D.; Lupini, A. R.; Pantelides, S. T.; Pennycook, S. J.; Kalinin, S. V.; Borisevich, A. Y. In Situ Observation of Oxygen Vacancy Dynamics and Ordering in the Epitaxial $LaCoO_3$ System. *ACS Nano* **2017**, *11* (7), 6942−6949.
(28) Lan, Q. Q.; Zhang, X. J.; Shen, X.; Yang, H. W.; Zhang, H. R.; Guan, X. X.; Wang, W.; Yao, Y.; Wang, Y. G.; Peng, Y.; Liu, B. G.; Sun, J. R.; Yu, R. C. Tuning the magnetism of epitaxial cobalt oxide thin films by electron beam irradiation. *Phys. Rev. Mater.* **2017**, *1*, 024403.
(29) Zhang, J.; Zhang, H.; Zhang, X.; Guan, X.; Shen, X.; Hong, D.; Zhang, H.; Liu, B.; Yu, R.; Shen, B.; Sun, J. Antiferromagnetic interlayer coupling and thus induced distinct spin texture for the $[LaMnO_3/LaCoO_3]_5$ superlattices. *Nanoscale* **2017**, *9* (10), 3476−3484.
(30) Zhang, J.; Chen, X.; Zhang, Q.; Han, F.; Zhang, J.; Zhang, H.; Zhang, H.; Huang, H.; Qi, S.; Yan, X.; Gu, L.; Chen, Y.; Hu, F.; Yan, S.; Liu, B.; Shen, B.; Sun, J. Magnetic Anisotropy Controlled by Distinct Interfacial Lattice Distortions at the $La_{1-x}Sr_xCoO_3/La_{2/3}Sr_{1/3}MnO_3$ Interfaces. *ACS Appl. Mater. Interfaces* **2018**, *10* (47), 40951−40957.
(31) Yang, H. W.; Zhang, H. R.; Li, Y.; Wang, S. F.; Shen, X.; Lan, Q. Q.; Meng, S.; Yu, R. C.; Shen, B. G.; Sun, J. R. Anomalous magnetism in strained $La_{1-x}Sr_xCoO_3$ epitaxial films ($0 \leq x \leq 0.5$). *Sci. Rep.* **2014**, *4*, 6206.
(32) Perdew, J. P.; Burke, K.; Ernzerhof, M. Generalized Gradient Approximation Made Simple. *Phys. Rev. Lett.* **1996**, *77* (18), 3865−3868.
(33) Egerton, R. F.; McLeod, R.; Wang, F.; Malac, M. Basic questions related to electron-induced sputtering in the TEM. *Ultramicroscopy* **2010**, *110* (8), 991−997.
(34) Ding, Y.; Pradel, K. C.; Wang, Z. L. In situ transmission electron microscopy observation of ZnO polar and non-polar surfaces structure evolution under electron beam irradiation. *J. Appl. Phys.* **2016**, *119* (1), 015305.
(35) Abbate, M.; Fuggle, J. C.; Fujimori, A.; Tjeng, L. H.; Chen, C. T.; Potze, R.; Sawatzky, G. A.; Eisaki, H.; Uchida, S. Electronic structure and spin-state transition of$LaCoO_3$. *Phys. Rev. B: Condens. Matter Mater. Phys.* **1993**, *47* (24), 16124−16130.
(36) Klie, R. F.; Zheng, J. C.; Zhu, Y.; Varela, M.; Wu, J.; Leighton, C. Direct measurement of the low-temperature spin-state transition in $LaCoO_3$. *Phys. Rev. Lett.* **2007**, *99* (4), 047203.
(37) Thornton, G.; Tofield, B. C.; Hewat, A. W. A Neutron Diffraction Study of $LaCoO_3$ in the Temperature Range 4.2 < T < 1248K. *J. Solid State Chem.* **1986**, *61*, 301−307.
(38) Hansteen, O. H.; Fjellvåg, H.; Hauback, B. C. Crystal Structure and Magnetic Properties of La2Co2O5. *J. Solid State Chem.* **1998**, *141*, 411−417.
(39) Hansteen, O. H.; Fjellvåg, H.; Hauback, B. C. Crystal structure, thermal and magnetic properties of $La_3Co_3O_8$. Phase relations for $LaCoO_{3-\delta}$ ($0.00 \leq \delta \leq 0.50$) at 673K. *J. Mater. Chem.* **1998**, *8* (9), 2081−2088.
(40) Zhang, H.; Zhang, J.; Yang, H.; Lan, Q.; Hong, D.; Wang, S.; Shen, X.; Khan, T.; Yu, R.; Sun, J.; Shen, B. Structural and Magnetic Properties of $LaCoO_3/SrTiO_3$ Multilayers. *ACS Appl. Mater. Interfaces* **2016**, *8* (28), 18328−33.
(41) Fuchs, D.; Pinta, C.; Schwarz, T.; Schweiss, P.; Nagel, P.; Schuppler, S.; Schneider, R.; Merz, M.; Roth, G.; V. Löhneysen, H. Ferromagnetic order in epitaxially strained $LaCoO_3$ thin films. *Phys. Rev. B: Condens. Matter Mater. Phys.* **2007**, *75*, 144402.

DOI: 10.1021/acs.inorgchem.9b02326
Inorg. Chem. 2019, 58, 13440−13445